RSC Advances

ROYAL SOCIETY OF CHEMISTRY

www.rsc.org/advances

This paper reports a new method developed to fabricate natural-rubber-based microfluidic devices (NRMDs) for optical and electrochemical applications.

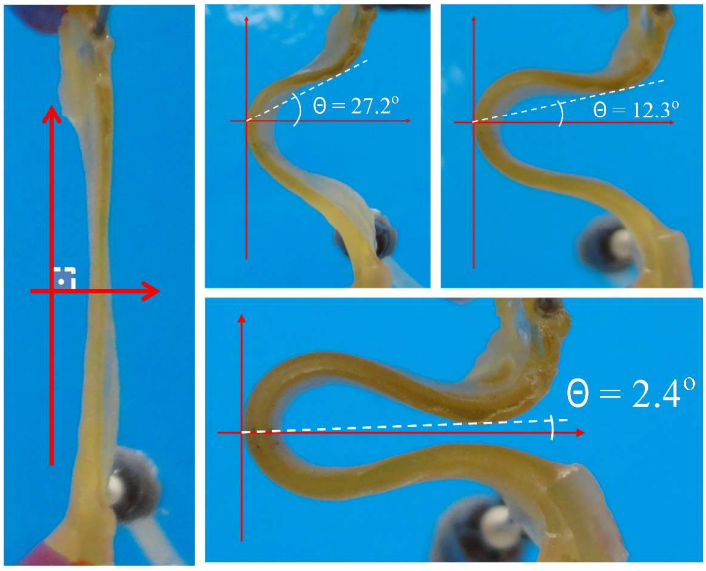

Journal Name RSCPublishing

ARTICLE

Natural-rubber-based flexible microfluidic device

Cite this: DOI: 10.1039/x0xx00000x

Flávio C. Cabrera,[a] João C. P. Souza,[b] Aldo E. Job[a] na d Frank N. Crespilho[*b]

Received 00th January 2012,
Accepted 00th January 2012

DOI: 10.1039/x0xx00000x

www.rsc.org/

Abstract

The fabrication of flexible devices is of great interest owing to their eco-friendliness, economic prospects, feasibility, and wide range of applications in biocompatible diagnostic devices and flexible labs-on-chips. Thus, this paper reports a new method developed to fabricate natural-rubber-based microfluidic devices (NRMDs) for optical and electrochemical applications. Furthermore, we provide a detailed protocol that will allow further study using NRMDs for the development of different lab-on-a-chip platforms. Microchannels were successfully replicated in NRMDs through casting of latex collected from trees of *Hevea Brasiliensis* into an acrylic moulding template. NRMDs combined both flexibility and transparency, the latter of which is an important characteristic for application in spectroscopic measurements in the visible range. When two flexible carbon fiber (FCF) electrodes were inserted into the NRMD, the device stated to work as a flexible electrochemical microcell. FCF electrodes showed a fast response to reach the stationary current immediately after the $[Fe(CN)_6]^{4-/3-}$ concentration was changed. High reversibility in the cleaning process was also confirmed when the microdevice was cleaned several times. Electronic spectroscopy was used to evaluating the absorption band of potassium 0.1 mol L^{-1} ferricyanide and results showed that NMRD is very efficient for spectroscopic analysis in flow. NRMDs with different formats and configurations were evaluated. The findings show that natural rubber is a robust and versatile promising material for building microfluidic labs-on-chips.

Journal Name RSCPublishing

ARTICLE

Introduction

Microfluidic technology allows laboratory tests to be performed on a miniature scale by manipulating fluids with precise volume control.[1–3] Miniaturisation offers microfluidic devices portability, consequently reducing the manufacturing cost as well as leading to decreases in material wastage as a result of low sample volume.[4] Moreover, microfluidic devices with control devices such as microvalves or micropumps integrated into their design can be self-contained. Challenges have been reported regarding the use of different fluid phases (gas–liquid) or viscosity (greater than 10^4 P), use of solid particles in suspension (cohesive and non-cohesive), as well as discovery of a new route to synthesise chemical or biological molecules depending entirely on the microfluidic technology used.[5] Systematic research studies on the use of microfluidic devices in areas such as point-of-care diagnosis,[6,7] immunoassays,[8,9] enzymatic assays,[10] plasmas,[11] DNA detection,[12] and cell manipulation[13,14] have recently been published. Furthermore, completely flexible microdevices that are composed of flexible electrodes have been reported for applications in biofuel cells.[15]

The development of flexible microfluidic devices allows the use of implantable biosensors to avoid the risk of a probe breaking as well as reduce the occlusion of fluidic channels. The flexibility also allows the devising of mechanisms to manipulate sample flow,[16] *e.g.* controlling flow rates with valves that can be used in switch-on/switch-off devices. Moreover, microfluidic technology using flexible supports have led to the improvement of flexible electronic systems,[17,18] as well as implantable devices that permit real-time measurements of physiological data, *e.g.* glucose or lactate level, neural activity.[19,20]

Nevertheless, the preparation of flexible microfluidic devices requires specific conditions. Most of the flexible devices are built using polymers which require precise settings (pH, temperature, viscosity, *etc.*) as well as specific preparation methods to obtain ideal properties. For example, some problems can be encountered during preparation of the moulding template or when determining the parameters of preparation such as temperature, time, *etc.* Consequently, the range of starting materials for the fabrication of microdevices has been extended by the use of polymers such as cyclic olefin copolymer (COC),[4] polymethylmethacrylate (PMMA),[11] poly(dimethylsiloxane) (PDMS),[12,15,21] and polyurethane methacrylate (PUMA),[22] as well as paper.[23] Most polymers used in microfluidic devices offer specific advantages like low cost, excellent mechanical properties, both easy fabrication and interfacing with other devices, transparency, environmental-friendliness, as well as biocompatibility. Natural rubber[24,25] is a unique material that combines every one of these properties, thus qualifying the elastomer *cis*-1,4-polyisoprene as a promising organic material for building flexible microdevices.

Soft elastomer, e.g. Ecoflex (silicone polymer), is of growing interest and an important strategy in the development of microfluidic device which require stretchability higher than the commonly used PDMS.[26] Moreover, the use of 'green materials' for the fabrication of flexible devices is of great interest owing to their eco-friendliness, economic prospects, feasibility, and wide range of applications in biocompatible diagnostic devices and flexible labs-on-chips.

Here we report the development of both flexible and organic microfluidic labs-on-chips. Channels were created on a flexible natural-rubber-based microfluidic device (NRMD) through casting of latex into an acrylic moulding template that contains the microdevice patterns. The fluid samples flowing inside the channels to the analysis window in the sensing chamber, where carbon fiber electrodes were placed, were responsible for the electrochemical assays. The main result shown here is the proof-of-concept that natural rubber can be used for building flexible microfluidic devices.

Materials and Methods

Self-standing natural-rubber microdevices were prepared using latex collected in a clean glass Erlenmeyer bottle from different rubber trees (*Hevea brasiliensis*) of the RRIM 600 clone (Fig. 1).

Fig. 1 Latex extracted from *Hevea brasiliensis* trees is collected in clean glass Erlenmeyer bottles on an experimental farm in the city of Indiana, São Paulo state. The latex samples were stabilised with ammonium hydroxide (2% v/v).

After extraction, latex samples were stabilised with ammonium hydroxide (2% v/v). Poly(vinyl chloride) (PVC) was acquired as a colourless liquid commercial adhesive based on the PVC resin. Flexible carbon-fiber (FCF) microelectrodes were extracted from a carbon cloth (CCS 200). The FCF electrodes were treated prior to processing using a solution consisting of 464.0 mg of H_2SO_4 in a 1.0 mol L^{-1} $KMnO_4$ solution, according to the procedure reported by Kovtyukhova *et al.*[27] In addition, 0.50 g of fibers was immersed in 120 mL of H_2SO_4/$KMnO_4$ under sonication for 3 h. Finally, the fibers were washed using a concentrated HCl solution to remove MnO_2 formed on the electrodes' surfaces. The fibers were also washed using distilled water to remove all acidic compounds. A solution of potassium ferricyanide ($K_3[Fe(CN)_6]$) in phosphate buffer (pH 7.0, 0.1 mol L^{-1}) was used in the

electronic spectroscopy experiments. The electrochemistry of the $[Fe(CN)_6]^{4-/3-}$ redox probe was also investigated. For this, experiments were carried out using an equimolar solution of $K_3[Fe(CN)_6]$ and $K_4[Fe(CN)_6]$ in phosphate buffer (pH 7.0, 0.1 mol L^{-1}).

The natural rubber was evaluated by stress–strain tests in which the sample was stretched at 500 mm/min using an EMIC DL2000 digital universal testing machine and using an internal deformation transducer. The sample preparation was carried out according to ASTM D412 type C. A peristaltic pump (Millifluidica SCMD-1008) and a syringe pump (KDS 100 series) were used to evaluate the microdevice's flow rate. The structural evaluation of the channels and sensing chamber reproduced in the natural rubber membrane's surface was recorded by a Biofocus BIO1600TA-L-BI optical microscope that was coupled to the chamber of the ocular digital lens MEM 1300 Digital Eyepiece. Scanning electron microscope (SEM) measurements were carried out using a Zeiss LEO 440 microscope (secondary electron detecting mode, operating at an accelerating voltage of 15.0 kV and a working distance of 9.0 mm). Visible-light absorption data was obtained using a Jasco V-670 spectrophotometer and an Avantes spectrophotometer (AvaLight-D(H)-S deuterium-halogen light sources) using an optical-fiber module. The electrochemical experiments were carried out in a potentiostat/galvanostat (Autolab PGSTAT204). The complete protocol for preparation of a natural-rubber microfluidic device is provided in Electronic Supplementary Information (ESI), as well as stress–strain text results of natural-rubber membrane, and absorbance and transmission spectra of natural-rubber membrane.

Results and Discussion

Fabrication of a flexible natural-rubber microdevice (NRMD)

The acrylic moulding template that contains the microdevice patterns is shown in Fig. 2.

The patterns were prepared using a permanent container made of acrylic in the shape of a rectangular box, with rounded corners to avoid changes in the die volume as a result of the fluid dynamics (Fig. 2a). Metallic cylinders were placed on the surface of the support to replicate the channels on the surface of the natural rubber. The final configuration of the flexible microfluidic device is shown in Fig. 2b. Four types of moulding templates are shown in Fig. 2c; different templates are used depending on the design of the microfluidic device, *e.g.* configuration IV is used to generate the interior of a mixer system with sinuous channels. Different materials such as glass, acrylic, and metal can be used to prepare the mould.

The procedure for replicating the channels and chamber in the flexible NRMD are also shown in Fig. 2. After the template preparation (patterns placed in acrylic box) (Fig. 2d), latex was released in drops into the box (Fig. 2e), covering the template. The latex-covered template was then submitted to thermal treatment (*i.e.* annealing) at 65 °C for 10 h (Fig. 2f). This was the minimum temperature selected to maintain the maximum transparency of the analysis window of the device.

A volume of 2.5 mL of latex was used to prepare each membrane. The drying time of latex was defined as the minimum time required to completely dry the entire natural-rubber surface. After the latex dried, the natural rubber membranes were removed from the moulding template replicating the open chamber and channels (Fig. 2g).

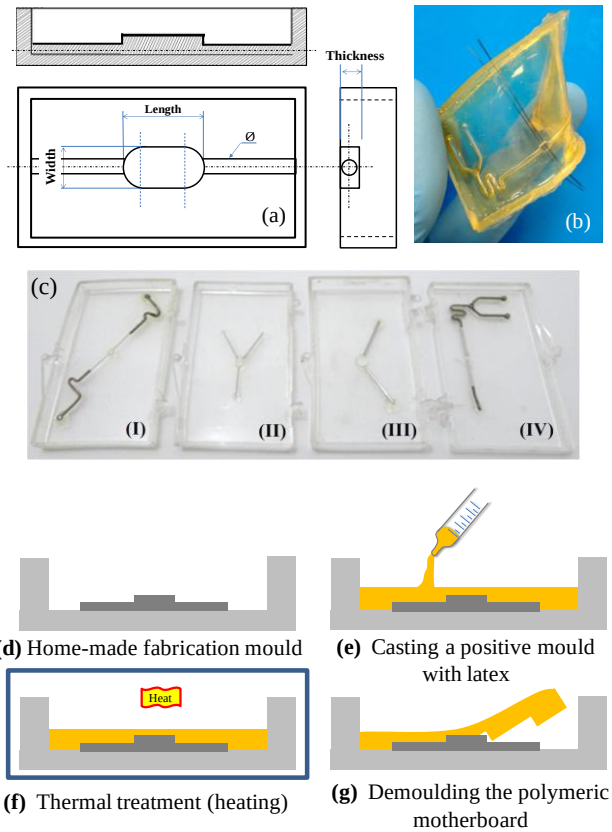

Fig. 2 (a) Scheme of the home-made acrylic moulding template with metallic cylinders to replicate the channels on a natural-rubber membrane. (b) Final configuration of the lab-on-a-chip (LOC). The carbon-fiber electrodes are above the analysis chamber. The natural rubber LOC is sealed with another thin natural rubber membrane using latex as the bonding material. (c) Different types of acrylic moulding templates used for replicating the configuration of the microfluidic device on the natural rubber surface. (d–g) Procedure for replicating both channels and chamber of the flexible NRMD. (d) Acrylic moulding template with the pattern of the chamber and channels. (e) Latex is released in drops into the container, covering the template. (f) Thermal treatment at 65 °C for 10 h to dry the latex forming the flexible NRMD. (g) Demoulding the natural rubber from the moulding template.

To build a microdevice for the electrochemistry experiments, electrodes were inserted over the analysis window and then sealed. The window area was sealed by releasing drops of latex over the surface around the chamber and channels. Another thin natural-rubber membrane with a thickness of 0.5 mm was placed on the surface of the flexible microdevice under manual pressure and then annealed at 65 °C for 2 h. Catheters were inserted in the channels (using cyanoacrylate adhesive) to configure the permanent inlet and outlet connectors. The complete protocol for preparation of a NRMD is provided in ESI. This documentation section provides step-by-step instructions for fabricating electrochemical device.

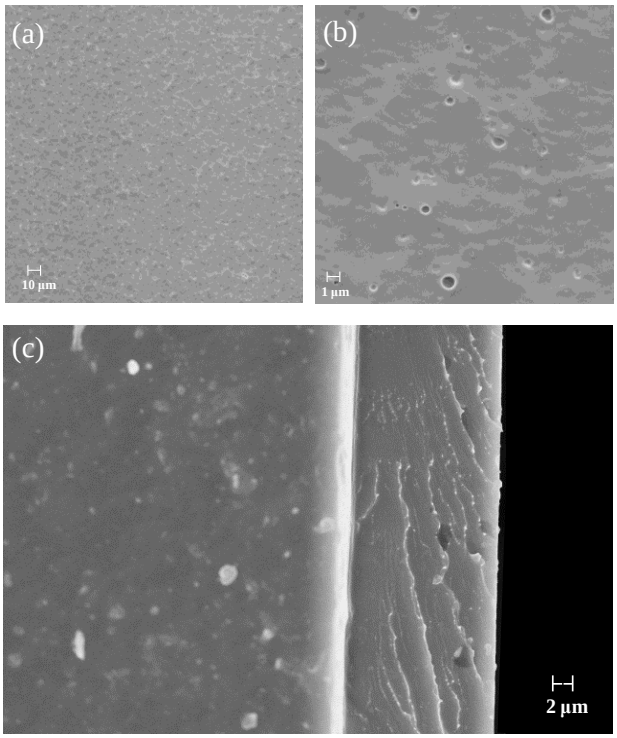

Fig. 3 PVC film (17.6 µm) covering the natural-rubber surface in order to increase that hydrophobic feature. Images under magnification of (a) 1,000 × and (b) 10,000 ×. (c) Cross-sectional analysis of the film.

Table 1 Parameters of the moulding template (relative to Figure 2a): width; length; thickness of analysis chamber window; diameter of cylinders used for replicating the channels on the natural rubber surface.

Natural-rubber microfluidic device				
Configuration	**Width (mm)**	**Length (mm)**	**Cylinder diameter (µm)**	**Analysis-window thickness (mm)**
I	1.8	1.9	150	0.2
II	2.0	3.0	300	0.6
III	3.4	3.7	700	1.0
IV	1.8	2.4	700	0.7

Table 1 summarises the dimensions of the template used to replicate different configurations of the channels as well as the size of chambers on the natural-rubber surface. Furthermore, the procedure implemented in our study can be compared to the prototype process for moulding a microfluidic foil device.[28] However, our procedure did not require the application of pressure to the mould or tools to demould the flexible NRMD.

Another important point is that by using a protective polymeric layer, the microchannels formed were compatible with hydrophobic coatings. Actually, the literature shown the natural rubber wettability based on measurement of contact angle around to 90-100°. [29,30] For instance, a 17.6-µm-thick hydrophobic PVC film was deposited on the internal surface of the flexible NRMD, as shown in Fig. 3.The PVC film was completely transparent, with good adherence on the natural rubber. Therefore, it was possible to observe that the PVC film covered the entire surface of the natural rubber.

Evaluating the NRMD flow rate

Optical microscope images of different configurations of a flexible natural-rubber microdevice are shown in Fig. 4. Linear and angular channels were built on the natural-rubber surface; configurations consisting of various combinations of these channels were also built. Three channel diameters were used: 142, 327, and 715 µm. Spiral channels with dimensions of around 665 µm were introduced, allowing the flow of solution between the spiral and linear channels. Spiral channels are supposed to be more efficient when building flow-mixer structures because of the larger contact surface area inside the channels. Although this study did not include the fabrication of NRMDs as mixers, we demonstrate here the possibility of configuring a microdevice for that application, as well as the possibility to identify the connections between the channels and analysis chamber.

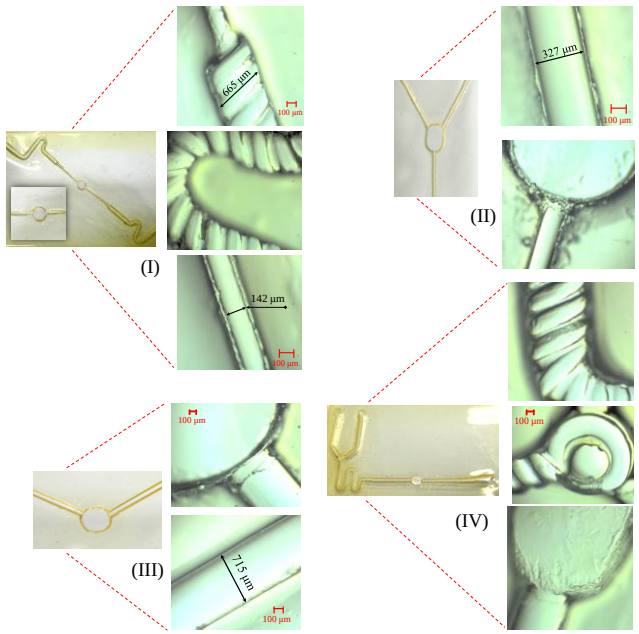

Fig. 4 Different configurations of a flexible lab-on-a-chip microdevice. Channels were built as linear and spiral pathways. (I) Device prepared with spiral channels with diameters of around 665.0 µm to transfer fluids to channels with diameters of around 142.0 µm and a chamber with a window thickness of 0.2 mm. (II) Device consisting of channels with diameters of around 327 µm and a chamber with a window thickness of 0.6 mm. (III) Device consisting of channels with diameters of around 715 µm and a chamber with a window thickness of 1.0 mm. (IV) Device prepared with spiral channels with diameters of around 665.0 µm to transfer fluids to channels with diameters of around 715.0 µm and a chamber with a window thickness of 0.7 mm.

The microfluidic properties (Fig. 5a) were evaluated, using the configuration I (Fig. 4), at inlet flow rates of 8 and 80 µL min^{-1}. The device's internal volume was measured to be 15 µL. The results for both high and low inlet flow demonstrate that the flow was continuous, *i.e.* the structure of the flexible device was not modified as a result of the flow (volume expansion, water absorption, channels obstructed, *etc.*). The flow rate was measured as a function of the angular deformation of the flexible device (Fig. 5b), which showed a tendency to decrease as the volume increased with deformation (the occluding angle decreased from 90° to around 2°) of the device (Fig. 5b(inset)). However, the flow rate variations were insignificant when

measurement errors were taken into consideration, which support the feasibility of the flexible microfluidic device. Measured values of the mechanical properties are shown in Fig. S1 (Supplementary Information). The phase of elastic deformation or limit of elasticity of the natural rubber membranes is defined on the curve of stress-strain tests from 0 to 125% of deformation (the membrane length reached after the stretching (125%) in this region is more than double when compared with the original length). Moreover, the tension of 0.45 MPa at a deformation of 125% is equivalent to the internal pressure of a device structure that is supported without permanent deformation. Hardness and axial deformation are measured by Young's modulus (E = 0.742 MPa), calculated in terms of the tension and deformation reached on the linear region observed in the stress-strain curves[31] (Equation I - Supplementary Information) as well as the Poisson's Rate (μ = 0.49994) which is calculated by relation of Young's modulus (E) and Bulk Modulus (K)[32] (Equation II - Supplementary Information), respectively. When the deformation was between 100 and 200%, the flow process of chains began just before the initial plastic deformation. The natural rubber membranes were capable of reaching a rupture tension of 1.0 MPa ± 0.2 (620% of deformation).

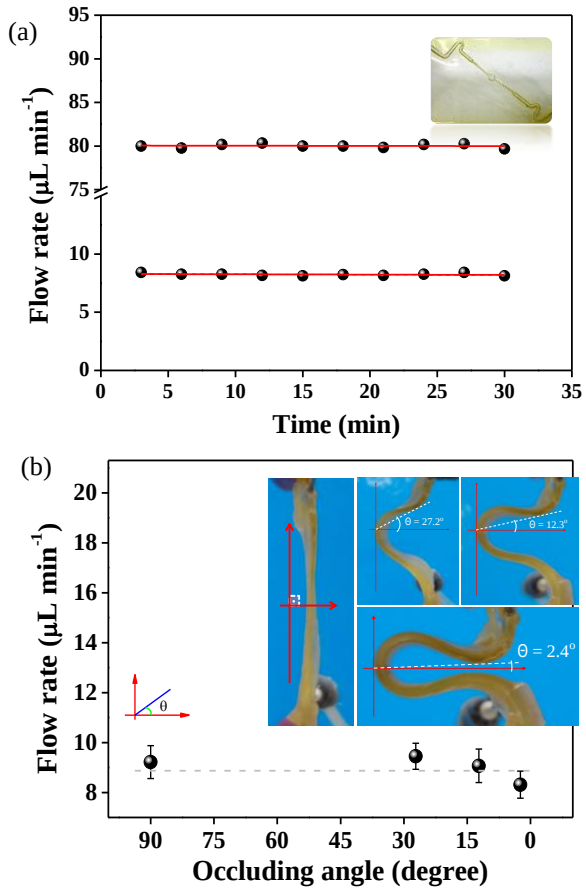

Fig. 5 (a) Flow rate evaluation using inlet flow rates of 8.3 and 80.0 μL min^{-1}. The microdevice configuration I (inset) was evaluated using a syringe pump to obtain the two flow rates, demonstrating that the flow was continuous (the deflection from the linear fit corresponded with the microbalance error). The internal volume of the microfluidic device was measured to be around to 15 μL. (b) Flow rate evaluation using an inlet flow rate of 9.8 μL.min^{-1}. The flow rate was evaluated at sensor angular deflections of 90°, 27.2°, 12.3°, and 2.4° (inset).

Evaluating the optical-based microfluidic device

In order to fabricate a flexible and transparent device, we used microfluidic device configuration I, which had a small analysis chamber (path length = window thickness = 0.2 mm) without the insertion of carbon electrodes into the optic window. The natural rubber did not absorb light in the visible spectrum and exhibited one absorption band around 280 nm that is attributed to protein compounds (Fig. S2, Supplementary Information). The working range of the absorption spectrum for natural rubber was evaluated through electronic spectroscopy (Fig. 6). The experiment was carried out by measuring the absorbance at the maximum wavelength of the absorption band (420 nm) and then comparing the value to the baseline (Fig. 6a) as the potassium ferricyanide concentration of the flowing solution increased (Fig. 6b).

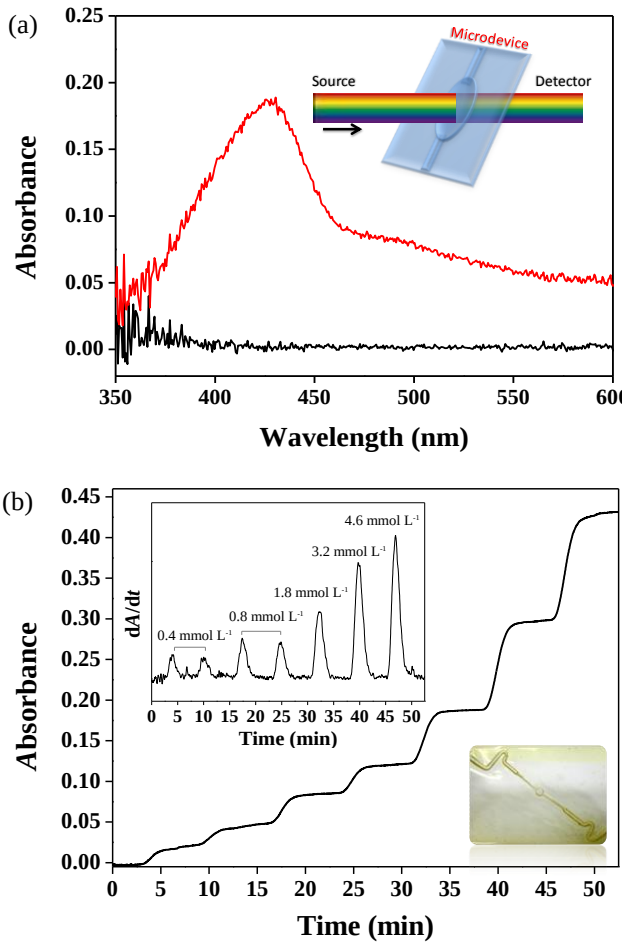

Fig. 6 (a) Electronic spectra obtained in a chamber window for 0.1 mol L^{-1} ferricyanide (red curve) and water (black curve). Inset: set-up illustration of the spectroscopy analysis showing the light passing through the device chamber. For this experiment, an optical-fiber was used (Avantes spectrophotometer AvaLight-D(H)-S deuterium-halogen light sources). (b) Absorbance–time transients for ferricyanide with several concentrations. Inset: first derivative of Fig. b. Flow rate: 80 μL min^{-1}(peristaltic pump). Concentrations: 0.4, 0.4, 0.8, 0.8, 1.8, 3.2, and 4.6, mmol L^{-1} (Jasco spectrophotometer, model V-670).

As shown in Fig. 6, electronic spectroscopy was used to evaluating the absorption band of potassium ferricyanide at 0.1

mol L^{-1} (red curve) compared to reference 50 measured on water (black curve) flowing into the chamber window. Fig 6a (inset) shows the schematic set-up of the spectroscopy analysis showing light passing through the device chamber using an optical-fiber module, where the incident light traversed the chamber in which the ferricyanide solution flow (flow rate: 80 µL min^{-1}) was maintained by a peristaltic pump. For each injection of ferricyanide solution, an increase was observed from the baseline of the spectrum. In $[Fe(CN)_6]^{3-}$, iron is in the d^5 configuration, which permits a charge transfer from the ligand to the metal. This phenomenon of charge transfer can be observed in the electronic region to the metal's t_{2g} level.[33,34] Therefore, the band at 420 nm in the electronic spectrum for ferricyanide is assigned to the charge transfer from the strong field ligand to the metal t_{2g} level. Moreover, as the concentration of ferricyanide in the flowing solution increased, absorbance peaks with similar relative intensities were observed (Fig. 6b) at the same concentration ratio, *e.g.* the peaks had similar intensities at 0.4 mmol L^{-1} and the peaks at 0.8 mmol L^{-1} had similar intensities. In other words, the solution was not absorbed on the chamber's interior walls under these conditions. These results demonstrate that the flexible NRMD can be implemented as photo-based microfluidic platforms, for instance, with application as a spectroscopic sensor.

Microfluidic for electrochemical devices

The flexibility of FCF electrodes was evaluated by manipulating a single fiber as well as a group of fibers into very small knots, as shown in Fig. 7a. The FCF electrodes displayed high conductivity as well as resistance to traction and bending, which improve the performance of the flexible microfluidic device by keeping the electrodes from breaking during continuous mechanical operation of the lab-on-a-chip device.

The FCF electrodes were inserted in the flexible NRMD to evaluate the microfluidic lab-on-a-chip as an electrochemical sensor using configuration IV. In fig. 7 (b and c), the cyclic voltammetry for 10.0 mmol L^{-1} $[Fe(CN)_6]^{4-/3-}$ at 100 mV s^{-1} is shown. Fig. 7b shows the voltammetry curve obtained for $[Fe(CN)_6]^{4-/3-}$ redox probe evaluation using Ag/AgCl as the reference electrode and the FCF electrodes as both working and counter electrodes. The following reactions represent the redox reactions attributed to the two voltammetry peaks at 0.2 V and 0.36 V, respectively:

$$[Fe(CN)_6]^{3-} + e^- \rightarrow [Fe(CN)_6]^{4-} \quad (1)$$

$$[Fe(CN)_6]^{4-} \rightarrow [Fe(CN)_6]^{3-} + e^- \quad (2)$$

The latter experiment was carried out again, however without Ag/AgCl reference electrode (Fig. 7c), and well-expected shift on both oxidation (0.13 V) and reduction (-0.14 V) peaks were observed. For this experiment, the reference electrode was placed on short-circuit with the counter electrode. This was done in order to obtain lab-on-a-chip with only two electrodes; a way to build a more robust device. Thus, device configuration IV (lower inset of Fig. 7d) was also implemented to evaluate the NRMD performance at different $[Fe(CN)_6]^{4-/3-}$concentrations (upper inset of Fig. 7d). The experiments were carried out as the concentration of the flow solution was increased in steps of equal proportions (Δc) to reach values of 0.4, 0.8, and 1.8 mmol L^{-1}, upper inset of Fig. 7d). The rate of change in current (dI/dt) responded at the same level of relative intensity for the same solution concentration, demonstrating the specificity (calibration) and reproducibility of the performance of the flexible carbon electrodes. The kinetics of the redox reaction were evaluated as the concentration was increased from 0.4 to 34.2 mmol L^{-1}, and the current response reached densities of 49 and 3392 µA cm^{-2}, respectively.

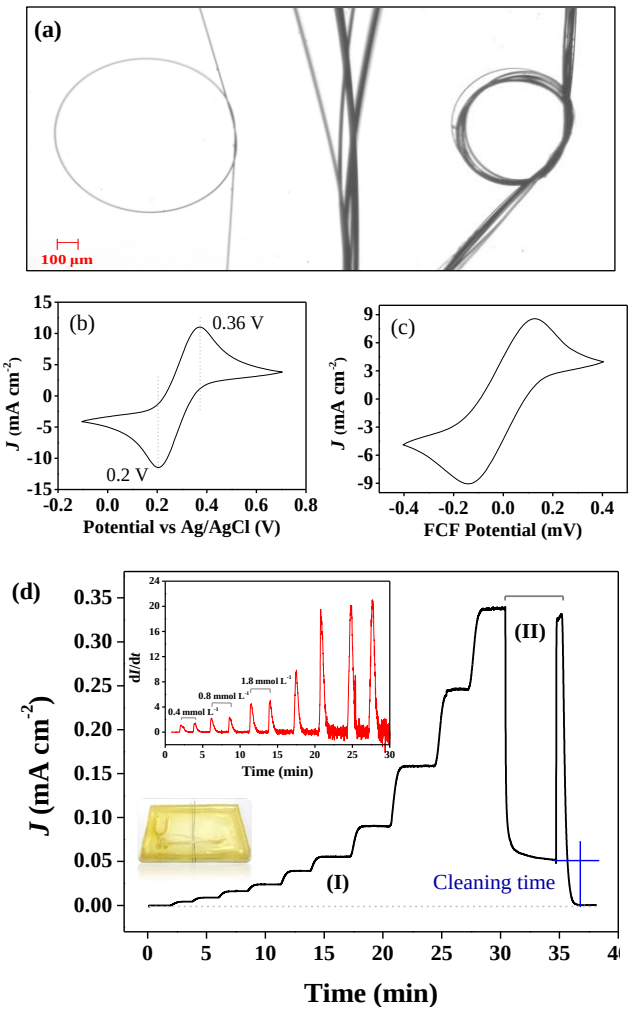

Fig. 7 (a) Optical microscope images showing the flexibility of different configurations of FCF electrodes. (b) Evaluation of the redox process for 10.0 mmol L^{-1} $[Fe(CN)_6]^{4-/3-}$ at 100 mV s^{-1}. The voltammetry was carried out using $Ag/AgCl_{sat}$ as the reference electrode and FCF as both working and counter electrodes. For this, a static flow of phosphate buffer solution at pH 7.0 was used as electrolyte support. (c) Cyclic voltammetry carried out in the same condition as described above, in (b); however the $Ag/AgCl_{sat}$ was not used. For this experiment, the reference electrode contact was placed on short-circuit with the counter electrode. (d) The configuration described above, in (c), was used to obtain the current–time transients plot using NRMD for evaluation of the redox process of $[Fe(CN)_6]^{4-/3-}$ in different concentrations: 0.4, 0.4, 0.8, 0.8, 1.8, 1.8, 3.5, 6.5, 8.3 and 9.7 mmol L^{-1}. Flow rate: 670 µL min^{-1}; applied potential: 0.13 V. Inset: photography of NRMD in configuration IV and a plot showing the reproducibility for several injections. For this, a first derivative was obtained from the data of current–time transients, using NRMD for evaluation of the redox process of $[Fe(CN)_6]^{4-/3-}$ at same concentrations described.

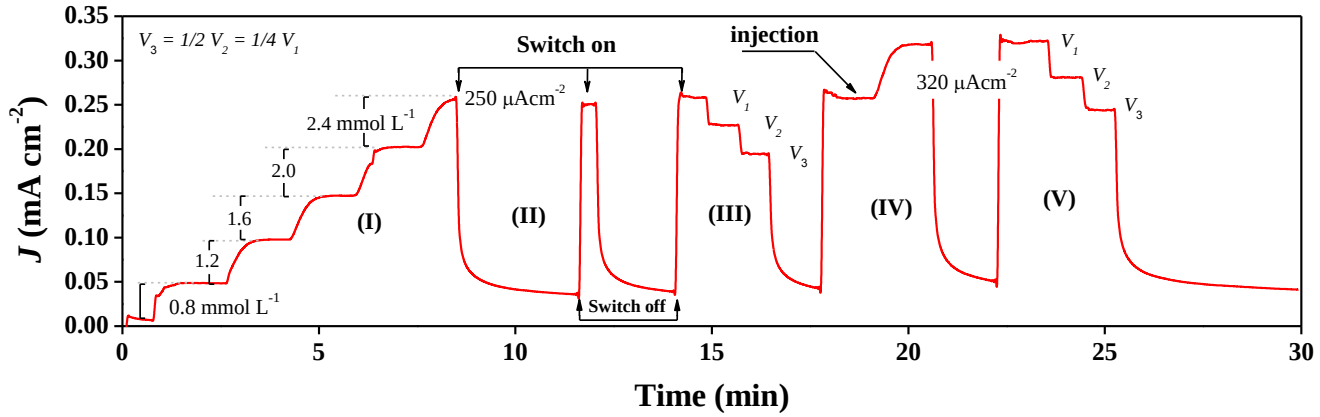

Fig. 8 Current–time transients (applied potential: 0.13 V) for evaluate the long-term stability of the NRMD. (I) Evaluation of different concentrations of $[Fe(CN)_6]^{4-/3-}$, in a range from 0.8 up to 2.4 mmol L^{-1} (initial concentration: 0.4 mmol L^{-1}). (II) Switch on/off of the peristaltic pump after reaching a current density of 250 µA cm^{-2}. (III) Evaluation of different inlet flow rates: V_1=670 µL min^{-1}, V_2= 335 µL min^{-1}, V_3= 167.5 µL min^{-1}. (IV) and (V) Test of reversibility of the system by repeating the analyses described for stages (I), (II), and (III).

In the second stage (II), we switched off the peristaltic pump to change the $[Fe(CN)_6]^{4-/3-}$ solution to a phosphate buffer solution (pH 7.0) in order to clean the system. After the flow of the solution was switched on, the current density increased, reaching a level similar to that before the flow solution was changed (3370 µA cm^{-2}), which is attributed to the volume of $[Fe(CN)_6]^{4-/3-}$ solution still present in the tubes connecting the peristaltic pump to the analysis chamber. However, less than 2 min was required to clean the entire system and revert to the initial condition before the electrode process began. The change in current-density with time was examined to determine the long-term stability of the device (Fig. 8), using an inlet flow rate of around 670 µL min^{-1}. In the first stage (I), we evaluated the reproducibility of the sensor operation and increased the solution concentration twice by the same amount, step-by-step, which demonstrated similar relative intensities of current, *i.e.* there were no accumulated species (reduced/oxidised) on the electrodes' surfaces, as was the case during electronic analysis. Moreover, the flexible electrode exhibited a fast response to reach a stationary current density immediately after changes were made to the $[Fe(CN)_6]^{4-/3-}$ concentration. The second stage (II) of the chronoamperometry curve demonstrated the reversibility of the device. During this stage, we switched off the peristaltic pump to evaluate the response from the carbon electrode, which exhibited the expected decrease on current density. Therefore, when the peristaltic pump was switched on, it was possible to notice that the curve returned to the same current density (if the inlet flow rate was unchanged). Furthermore, different inlet flow rates could be tested by changing only the absorption relative intensity, *i.e.* the electrochemistry characteristics were unaffected, as demonstrated in the third stage (III), and the results for three different proportional inlet flow rates were reproduced. Posterior changes to the flow concentration demonstrated that even after cycling tests, the electrodes continued to work (stages IV and V). The system resilience is noted as a result of the brief time (around 25 min) spent on numerous tests using a high flow rate.

Discussion

The main result shown here is the proof-of-concept that natural rubber can be used for building flexible microfluidic devices. The detailed experimental procedure is described in the supplementary information, in the section *protocol for NRMD fabrication*. The procedure begins with the extraction process to obtain latex rubber from *Hevea brasiliensis* trees (Fig. 1). At this stage, as latex coagulates quickly when exposed to air, stabilisation using ammonium hydroxide is necessary. As a result, extraction commonly takes place in the mornings to slow down the accelerated coagulating reaction resulting from high temperature. The process of latex stabilisation can be explained by the current model proposed for the structure of latex rubber particles. Moreover, the principle of the model is that the latex particles are formed by a core–shell structure consisting of isoprene molecules in the core enclosed by proteins and phospholipids linked to terminal chain groups.[35] These particles present amino-functional groups that can be stabilised by charge interactions when ammonium hydroxide is inserted.

In our study, the stabilised latex was used to prepare the natural rubber motherboard, *i.e.* the polymeric support of the microfluidic device, through a thermal process. The template was built using acrylic and metal cylinders, although other materials which support the temperature used and are not reactive to ammonium–latex could be implemented. It is essential to use an oven with high temperature precision that demonstrates internal homogeneity of heating and temperature stability, which can be improved by forced-air circulation. A slow rate of heating and cooling is also important to obtaining a homogeneous polymer surface. Increasing the temperature of thermal treatment decreases the transparency of the polymeric device, which can also be modified by increasing the thickness of the natural-rubber membrane. Based on this fact, we evaluated the temperatures that offered better results and determined that 65 °C was the optimal temperature for the preparation of the natural-rubber motherboard. Furthermore, the duration of the thermal treatment can vary proportionately with the amount of water in the latex composition. Although it is necessary to control some of the parameters, the process of preparation of both the mould template and natural-rubber motherboard are relatively simple and inexpensive, and it does not require expensive devices or in-depth knowledge of the process or polymer manipulation. Also, natural rubber offers the possibility of adding coating layers of hydrophobic/hydrophilic materials such as PVC, which allows the implementation of new properties and new applications of the microfluidic device.

In addition, the main goal of proposing NRMDs is to obtain a completely flexible lab-on-a-chip, without losing the properties during successive application of mechanical stress through the use of flexible carbon fibers (Fig. 7) as electrodes, as shown in Fig. 5b. It was observed that the flow rate remained almost unchanged during mechanical deformation, where the internal angular deflection reached almost 360° in the last stage, as shown in the inset of Fig. 5.

The optic properties were evaluated in this study using the ferricyanide solution that exhibited an absorption band in the visible spectrum; evaluation of the electrochemical properties allowed the study of the kinetics of the reaction. Moreover, it was possible to observe the latex transparency in the visible region, allowing the identification of the ferricyanide bands shown in Fig. 6. The effect of different ferricyanide concentrations was evaluated by electrochemical tests, which demonstrated the reproducibility of the change in absorbance intensity when the concentration of ferricyanide in the flowing solution was increased stepwise by the same amount.

The reversibility in the cleaning process was also confirmed when the microdevice was cleaned several times (in less than two minutes depending on the inlet flow rate), showing that there were no accumulated species (reduced/oxidised) on the electrodes' surfaces. Furthermore, the FCF works as a flexible sensor, showing a fast response to reach the stationary current immediately after the $[Fe(CN)_6]^{4-/3-}$ concentration was changed. Currently, FCFs are intensively studied by our research group[36-40] because of its high conductivity and flexibility as well as the fact that carbon fibers are made from pure materials, which decreases the interference on measurements from structural defects or impurities. In addition, we believe that both the micromanipulation and modification of FCFs surface are possible ad promising for application in NRMD. Also, FCF functionalization and immobilization of different components (mediators, enzymes, organic molecules, and nanostructures) allows the implementation of specific properties for new electrodes generations applied in NRMD.

Conclusions

In this work, a novel concept of microscale labs-on-chips for optical and electrochemical microfluidic devices was presented. Our results showed the flexibility of a microfluidic device without interfering with the fluid flow rate. Channels were well replicated in the flexible NRMD by casting latex in an acrylic moulding template that contains the microdevice patterns. The findings show that natural rubber is a promising material for building microfluidic labs-on-chips.

Keywords: Microfluidic device; carbon fiber electrode; natural rubber; flexible device; lab-on-a-chip.

Acknowledgements

The authors gratefully acknowledge Brazilian agencies for financial support in their research activity, including FAPESP (F.N. Crespilho projects numbers: 2013/14262-7 and 2013/04663-4); CNPq (F.N. Crespilho project numbers: 306106/2013-2 and 478525/2013-3), INEO, and Nanomedicine Networks (NanoBio-Net and NanoBioMed-Brazil, CAPES). F.C. Cabrera acknowledges FAPESP (Doctoral Fellowship number 2011/23362-0) for support.

Notes and references

[a] *A Faculdade de Ciências e Tecnologia FCT/UNESP, Departamento de Física, Química e Biologia, Presidente Prudente, SP, Brasil.*
[*b] *Universidade de São Paulo, Instituto de Química, São Carlos, SP, Brasil.* frankcrespilho@iqsc.usp.br

† Electronic Supplementary Information (ESI) available: Stress–strain text results of natural-rubber membrane; absorbance and transmission spectra of natural-rubber membrane; complete protocol for preparation of a natural-rubber microfluidic device. See DOI: 10.1039/b000000x/

1 D. Mark, S. Haeberle, G. Roth, F. von Stetten and R. Zengerle, *Chem. Soc. Rev.*, 2010, **39**, 1153–1182.
2 Y. C. Lim, A. Z. Kouzani and W. Duan, *Microsyst. Technol.*, 2010, **16**, 1995–2015.
3 L. Y. Yeo, H.-C. Chang, P. P. Y. Chan and J. R. Friend, *Small*, 2011, **7**, N. 1, 12–48.
4 C. H. Ahn, J.-W. Choi, G. Beaucage, J. H. Nevin, J.-B. Lee, A. Puntambekar and J. Y. Lee, *Proc. IEEE*, 2004, **92**, N. 1,154–173.
5 K. S. Elvira, X. C. i Solvas, R. C. R. Wootton and A. J. deMello, Nature Chem., 2013, **5**, 905–915.
6 V. Gubala, L. F. Harris, A. J. Ricco, M. X. Tan and D. E. Williams, *Anal. Chem.*, 2012, **84**, 487–515.
7 A. M. Foudeh, T. F. Didar, T. Veresa and M. Tabrizian, *Lab Chip*, 2012, **12**, 3249–3266.
8 M. S. Chiriacó, E. Primiceri, E. D´Amone, R. E. Ionescu, R. Rinaldi and G. Maruccio, *Lab Chip*, 2011, **11**, 658–663.
9 M. Lee, K. Lee, K. H. Kim, K. W. Oh and J. Choo, *Lab Chip*, 2012, **12**, 3720–3727.
10 D. N. Kim, Y. Lee and W-G Koh, *Sens. Actuators, B*, 2009, **137**, 305–312.
11 H. Sakamoto, R. Hatsuda, K. Miyamura and S. Sugiyama, *Micro Nano Lett.*, 2012, **7**, I. 1, 64–67.
12 S. K. Chhina, C. F Perez and M. Parameswaran, *J. Micromech. Microeng.*, 2012, **22**, 115038.
13] C.-H. Chuang, Y.-W. Huang and Y.-T. Wu, *Biomed. Microdevices*, 2012, **14**, 271–278.
14 L. M. Davis, J. L. Lubbeck, K. M. Dean, A. E. Palmer and R. Jimenez, *Lab Chip*, 2013, **13,** 12, 2320–2327.
15 T. Moriuchi, S. Sumida, A. Furuya, K. Morishima and Y. Furukawa, *Int. J. Precis. Eng. Manuf.*, 2009, **10**, N. 1, 75–78.
16 Y. C. Lim, A. Z. Kouzaniand and W. Duan, *Microsyst. Technol.*, 2010, **16**, 1995–2015.
17 P. K. Yuen and V. N. Goral, *Lab Chip*, 2010, **10**, 384–387
18 B. Zhang, Q. Dong, C. E. Korman, Z. Li and M. E. Zaghloul, *Sci. Rep.*, 2013, **3**, 1098,1–8.
19 R. Kuritaa, K. Hayashib, X. Fanc, K. Yamamotoc, T. Katod and O. Niwa, *Sens. Actuators, B*, 2002, **87** , 296–303
20 S. T. Retterer, K. L. Smith, C. S. Bjornsson, J. N. Turner, M. S. Isaacson and W. Shain, *J. Neural Eng.*, 2008, 5, 385–391.
21 W. Song, A. E. Vasdekis and D. Psaltis, *Lab Chip*, 2012, **12**, 3590–3597.
22 J. Alvankarian and B. Y. Majlis, *J. Micromech. Microeng.*, 2012, **22,** 035006.
23 A. W. Martinez, S. T. Phillips and G. M. Whitesides, *Proc. Natl. Acad. Sci. U. S. A.*, 2008, **105**, N. 50, 19606–19611.
24 F. Mrué, J. C. Netto, R. Ceneviva, J. J. Lachat, J. A. Thomazini and H. Tambelini, *Mater. Res.*, 2004, **7**, N. 2, 277–283.
25 M. Ferreira, R. J. Mendonça, J. Coutinho-Netto and M. Mulato, *Braz. J. Phys.*, 2009, **39**, N. 3.
26 M. Kubo, X. Li, C. Kim, M. Hashimoto, B. J. Wiley, D. Ham and G. M. Whitesides, Adv. Mater. 2010, **22**, 2749–2752.
27 N. I. Kovtyukhova, P. J. Ollivier, B. R. Martin, T. E. Mallouk, S. A. Chizhik, E. V. Buzaneva and A. D. Gorchinskiy, *Chem. Mater.*, 1999, **11**, 771–778.

28 M. Focke, D. Kosse, C. Muller, H. Reinecke, R. Zengerle and F. von Stetten, *Lab Chip*, 2010, **10**, 1365–1386.

29 S. Schlögl, R. Kramer, D. Lenko, H. Schröttner, R. Schaller, A. Holzner and W. Kern. *European Polymer Journal*, 2011, **47**, 2321–2330.

30 W. Anancharungsuk, S. Tanpantree, A. Sruanganurak, and P. Tangboriboonrat. *Journal of Applied Polymer Science*, 2007, **104**, 2270–2276.

31 J. R. White and S. K. De (Edits.). Rubber Technologist's Handbook. Chapter 10, Testing, R. Brown, 311-349, Rapra Technology Limited, UK, 2001, ISBN: 1-85957-262-6.

32 J. Brandrup and E. H. Immergut (Edits.) Polymer Handbook, John Wiley and Sons, New York, Chapter. V, Physical Constants of Different Rubbers, Lawrence A. Wood, 7-13, 1975.

33 J. J. Alexander and H. B. Gray, *J. Am. Chem. Soc.*, 1968, **90,** 16, 4260-4271

34 S. Radha and P. V. Kamath, *Bull. Mater. Sci*., 2013, **36,** 5, 923–929.

35 K. Nawamawat, J. T. Sakdapipanich, C. C. Ho, Y. Ma, J. Song and J. G. Vancso, *Colloids Surf., A*, 2011, **390**, 157–166.

36 G. M. Olyveira, J. H. Kim, M. V. A. Martins, R. M. Iost, K. N. Chaudhari, J.-S. Yu, and F. N. Crespilho, Journal of Nanoscience and Nanotechnology, 2012, **12**, 356–360.

37 F. C. P. F. Sales, R. M. Iost, M. V. A. Martins, M. C. Almeida and F. N. Crespilho, Lab Chip, 2013, **13**, 468–474.

38 M. V. A. Martins, A. R. Pereira, R. A. S. Luz, R. M. Iost, and F. N. Crespilho, Phys. Chem. Chem. Phys, 2014, DOI: 10.1039/c4cp00452c.

39 R. A. S. Luz, A. R. Pereira, J. C. P. de Souza, F. C. P. F. Sales, and F. N. Crespilho, Journal Chem. Electro. Chem., 2014, DOI: 10.1002/celc.201402141.

40 O. N. Oliveira Jr., R. M. Iost, J. R. Siqueira Jr., F. N. Crespilho, and L. Caseli, ACS Appl. Mater, 2014, DOI: 10.1021/am5015056.